



## Subdiffraction fluorescence imaging of biomolecular structure and distributions with quantum dots

Meike Heidbreder<sup>a</sup>, Ulrike Endesfelder<sup>a</sup>, Sebastian van de Linde<sup>a</sup>, Simon Hennig<sup>a</sup>, Darius Widera<sup>b</sup>, Barbara Kaltschmidt<sup>c</sup>, Christian Kaltschmidt<sup>b</sup>, Mike Heilemann<sup>a,\*</sup>

<sup>a</sup> Applied Laser Physics and Spectroscopy, Physics Department, Bielefeld University, Universitätsstrasse 25, 33615 Bielefeld, Germany

<sup>b</sup> Cell Biology, Bielefeld University, Universitätsstrasse 25, 33615 Bielefeld, Germany

<sup>c</sup> Molecular Neurobiology, Biology Department, Bielefeld University, Universitätsstrasse 25, 33615 Bielefeld, Germany

### ARTICLE INFO

#### Article history:

Received 25 April 2010

Received in revised form 10 June 2010

Accepted 11 June 2010

Available online 23 June 2010

#### Keywords:

Fluorescence microscopy

Superresolution

Quantum dot triexciton imaging

TNF receptor

Mitochondrial inner membrane

### ABSTRACT

We introduce semiconductor quantum dot-based fluorescence imaging with ~2-fold increased optical resolution in three dimensions as a method that allows both studying cellular structures and spatial organization of biomolecules in membranes and subcellular organelles. Target biomolecules are labelled with quantum dots via immunocytochemistry. The resolution enhancement is achieved by three-photon absorption of quantum dots and subsequent fluorescence emission from a higher-order excitonic state. Different from conventional multiphoton microscopy, this approach can be realized on any confocal microscope without the need for pulsed excitation light. We demonstrate quantum dot triexciton imaging (QDTI) of the microtubule network of U373 cells, 3D imaging of TNF receptor 2 on the plasma membrane of HeLa cells, and multicolor 3D imaging of mitochondrial cytochrome *c* oxidase and actin in COS-7 cells.

© 2010 Elsevier B.V. All rights reserved.

### 1. Introduction

Fluorescence microscopy is a versatile tool in biomedical research as it is noninvasive, specific, very sensitive, and compatible to experiments in living cells, tissue, or even organisms. In the past decades, a variety of fluorescence microscopes became commercially available that are facile to use and easily accessible for nonexperts, such that fluorescence microscopy has entered many research areas. However, as any lens-based light microscopy technique, fluorescence microscopy is limited in its spatial resolution to about 200 nm in the focal plane and >500 nm along the optical axis. In the recent past, a new branch of fluorescence microscopy emerged that developed strategies to bypass the inherent resolution limit of light microscopy [1,2], motivated by the need to perform microscopy at biomolecular length scales of some nanometres and to achieve even near-molecular optical resolution [1].

A large set of fluorescence methods that achieve superior optical resolution have been developed in the past years. These methods are different in the underlying principle used to generate a super-resolution image, in the achievable spatial resolution and the demand

for specific labels [1–4]. Some methods have demonstrated to work in living cells [3,5] or even at video rate [6,7,24]. It is, however, the technical complexity and mathematical demand, together with expensive instrumentation, that often obviates a general use of these methods in everyday research. This is particularly true in research areas that would profit the most from imaging techniques with superior resolution and usually are nonspecialists in advanced and complex microscopy, i.e., biomedical research.

Very recently, we have introduced a method that enables ~2-fold optical resolution in 3D using semiconductor quantum dots as fluorescent labels [8]. This method can be implemented on any confocal microscopic system that is equipped with continuous-wave excitation in a spectral region of 450 nm to 550 nm, e.g., argon ion laser sources. The underlying physical phenomenon that finally leads to the resolution enhancement is a multiphoton absorption of semiconductor quantum dots. Specifically, a triple excitonic (triexcitonic) state is generated upon recombination emits blue-shifted fluorescence light, which is well separable from the “conventional” emission signal of the quantum dots. Different from conventional two- or multiphoton microscopy where virtual levels come into play and require the use of infrared excitation light and short laser pulses to provide the necessary intensity within the short lifetime of the virtual states, multiexcitons in quantum dots can be excited subsequently and with visible light. Furthermore, and again different from the very short-lived virtual levels in multiphoton microscopy, the individual excitons exhibit lifetimes that are long enough that

\* Corresponding author. Applied Laser Physics and Laser Spectroscopy, Bielefeld University, Universitätsstr. 25, 33615 Bielefeld, Germany. Fax: +49 521 106 2958.

E-mail address: [heileman@physik.uni-bielefeld.de](mailto:heileman@physik.uni-bielefeld.de) (M. Heilemann).

URL: <http://www.physik.uni-bielefeld.de/mh> (M. Heilemann).

conventional continuous-wave laser sources instead of short-pulsed (and expensive) laser sources can be used. In summary, the beauty of the concept lies in its very easy implementation on conventional microscopes, literally requiring a simple change in filter settings to achieve the resolution enhancement.

Here, we apply quantum dot triexciton imaging (QDTI) [8] to study the biomolecular structure and spatial organization in cells with subdiffraction spatial resolution. The benefit of using this concept lies in both the superior spatial resolution in 3D as well as the optical sectioning along the *z*-axis, which significantly reduces out-of-focus light. We demonstrate 3D imaging of proteins organized on cell membranes or subcellular organelles and simple approaches for quantitative analysis of protein distributions. Finally, we demonstrate how QDTI can be combined with organic fluorophores for multicolor confocal microscopy.

## 2. Experimental

### 2.1. Cell culture

U373 cells (human, glioblastoma–astrocytoma), HeLa cells (human, epithelial carcinoma), and COS-7 cells (derivative of the simian CV1) were grown in DMEM/F12 (High-Glucose; Gibco) containing 10% fetal calf serum (Gibco). Fresh medium was provided every second day. All cultures were incubated at 37 °C and 5% CO<sub>2</sub>. For staining experiments, cells were trypsinized and transferred into Lab-Tek chamber slides (Nunc) and grown at 37 °C and 5% CO<sub>2</sub> until adhesion was re-established.

### 2.2. Fixation

Cells were fixed with 4% paraformaldehyde (Sigma) in phosphate-buffered saline (PBS; Fluka) for 10 minutes at 37 °C. Cells were then washed with PBS and permeabilised with PBS containing 0.05% Triton X-100 (Sigma) for 10 minutes, then blocked with PBS containing 5% bovine serum albumin (BSA; Sigma) or 5% normal goat serum (NGS; Sigma) for 60 minutes at 37 °C. After washing with PBS containing 0.05% Triton X-100, cells were stained with antibodies.

### 2.3. TNFR2 and microtubule antibody stain

TNFR2 receptors were stained using anti-TNFR2 antibody (mouse anti-human; Axxora) or microtubules with anti- $\beta$ -tubulin antibody (mouse anti-human; Invitrogen) for 1 hour. Cells were washed with PBS and then stained with QDot655 (goat anti mouse F(ab')<sub>2</sub>; Invitrogen) at room temperature overnight. After washing with PBS containing 0.05% Triton X-100, nuclei were stained with Sytox Blue nucleic acid stain (Invitrogen) for 20 minutes. After washing with

PBS, cells were embedded in Mowiol (Sigma) and stored at room temperature.

### 2.4. Cytochrome *c* oxidase antibody and actin stain

To stain cytochrome *c* oxidase of mitochondria, COS-7 cells were incubated with anti-OxPhos Complex IV subunit I antibody (mouse monoclonal; Invitrogen) for 1 hour. Actin was stained with Alexa Fluor 488 phalloidin (Invitrogen) together with the first antibody.

Afterwards cells were stained overnight at 4 °C with secondary antibodies carrying QDot655 (goat anti mouse F(ab')<sub>2</sub>; Invitrogen). Three washing steps using PBS containing 0.1% vol./vol. Tween 20 (Sigma) were performed after each staining step. The cells were kept in PBS and were measured directly after the last staining step.

### 2.5. QDTI imaging

QDTI imaging was realized using a commercial confocal laser scanning microscope (LSM 710; Carl Zeiss, Jena, Germany) and analyzed using the ZEN2008 software (Carl Zeiss, Jena, Germany). Excitation wavelengths used were 488 nm and 458 nm, and emission windows were set at 580 to 620 nm (triexciton channel) and 650 to 720 nm (monoexciton and biexciton channels). Spectral separation on two detectors (photomultiplier tubes) was achieved by selecting a dichroic beam splitter (633 nm), and both detectors were operated at the same gain. Excitation powers were set to reach equal fluorescence signals on both detectors to ensure best comparability in terms of resolution increase. Typically, a 10-fold higher intensity was used for triexciton imaging. Pixel sizes of 40 to 100 nm (lateral) and 150 to 250 nm (axial) were used, and the pinhole diameter was set to 40 to 65  $\mu$ m.

### 2.6. Image analysis

Image analysis was performed using ImageJ (NIH) and the “3D objects counter” plug-in. The algorithm was first tested on individual quantum dots adsorbed on glass and imaged in the triexciton channel. The approximate dimension of the point-spread function (PSF) under different imaging conditions (pixel size, pinhole, excitation intensity) was determined, and parameters to discern close-by quantum dots were estimated. Cell images were then analyzed using suitable values for intensity threshold and appropriate spot size (matching the experimental PSF of QDTI).

## 3. Results and discussion

Fluorescence microscopy of quantum dot-labelled biomolecules was performed with commercially available QDot655 (Invitrogen) on

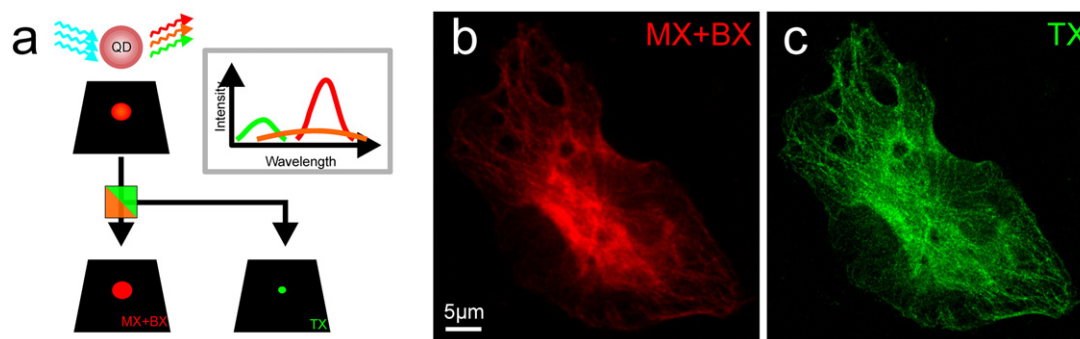


**Fig. 1.** (a) QDTI is realized by exciting semiconductor quantum dots QDot655 with 488 nm. As a consequence of multiexciton generation, three excitonic states with different fluorescence emission characteristics are generated. The emission of the triexciton is blue-shifted and can be spectrally separated. As a consequence of the three-photon absorption, the size of the point-spread function (PSF) is reduced  $\sim$ 2-fold, a measure of resolution enhancement. (b, c) Confocal fluorescence images of U373 cells, microtubule network stained by immunofluorescence using secondary antibodies labelled with QDot655. The triexciton channel (c) shows an increase in resolution and less contribution of out-of-focus light (optical sectioning).

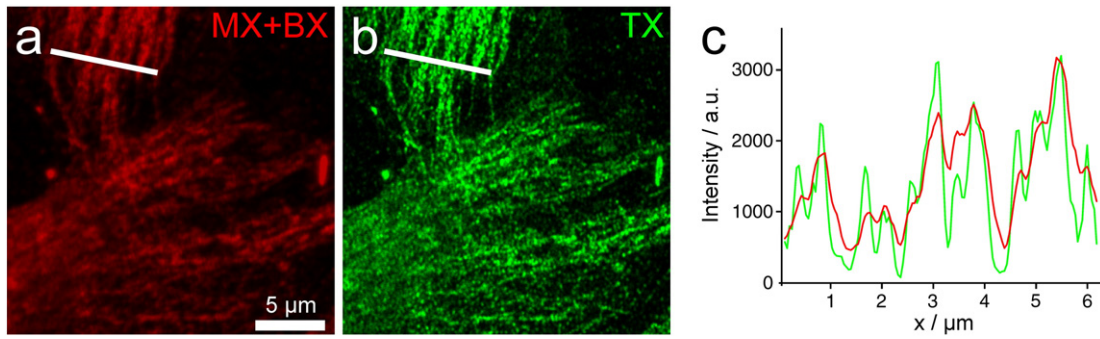


**Fig. 2.** (a, b) QDTI fluorescence images of microtubules in U373 cells, using a pixel size of 44 nm exhibits higher optical resolution in the triexciton channel (b), which is corroborated by the line profiles (c) of the fluorescence intensity. Clearly, the filamentous structure of microtubules is better resolved in the TX channel (green).

a conventional confocal microscope equipped with various continuous-wave laser sources (LSM710; Zeiss). In classical fluorescence experiments with QDot655, the quantum dots are excited at a wavelength of 635 nm, and the fluorescence emission is observed to peak at 655 nm. The photon absorption of a quantum dot leads to the formation of an electron–hole pair (“exciton”) that, upon recombination, emits fluorescence. Because of the unique photophysical properties of quantum dots, i.e., a very broad excitation spectrum that spans into the deep UV region, QDot655 can also be excited at any wavelength below 635 nm. Higher excited states or multiexcitonic states have been reported for quantum dots previously [9–11] and required the use of blue-shifted excitation wavelengths. Using laser light excitation at 488 nm, for example, triple-excitonic (triexcitonic) states can be generated in QDot655 quantum dots following the

absorption of three photons. These three excitonic states exist in parallel and recombine one after the other, each leading to the emission of a photon. The recombination of the monoexcitonic (MX) state occurs at the energy that corresponds to the conventional emission of the QDot655 quantum dots and overlaps with the emission of the biexcitonic (BX) state that is slightly red-shifted and cannot be spectrally separated [10]. The emission of the triexciton (TX) is spectrally shifted by ~60 nm to higher energy (shorter wavelength) and can easily be separated by setting the emission window properly (Fig. 1a). As a result of a three-photon absorption process, the point-spread function (PSF) in the triexciton channel is squeezed by a factor of 3 in theory. Experimentally, a resolution enhancement in 3D of ~2 was determined by measuring the PSF of single quantum dots in a polymer matrix [8]. The factor by which the PSF is squeezed is a

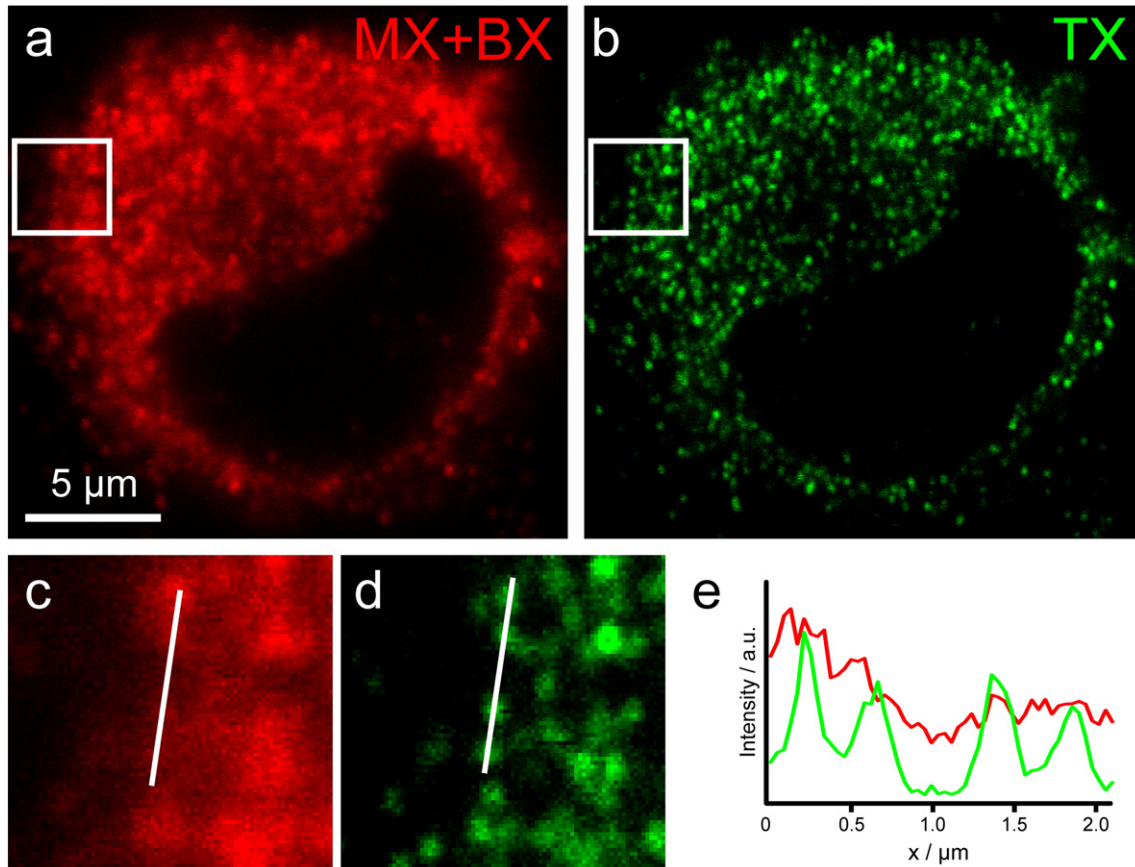


**Fig. 3.** (a, b) Confocal fluorescence images of TNF receptor 2 in HeLa cell. The resolution of single receptors in the triexciton channel is further demonstrated in the magnified view and the intensity line profile. Note the clear punctated staining; the grade of separation of isolated immunopositive structures is evident in the line profile.

measure for the resolution enhancement in all three dimensions for quantum dot three-exciton imaging (QDTI) [8]. A similar concept separating MX and BX emission of quantum dots using pulsed excitation has been published recently [12].

The QDTI concept can be applied to fluorescence microscopy of biomolecular structures in cells, such as the microtubule network (Figs. 1b and c). U373 cells were labelled by immunofluorescence using a primary antibody against  $\beta$ -tubulin and a QDot655-labelled secondary antibody fragment. The fluorescence signal was recorded on the conventional emission channel (Fig. 1b), and the TX channel (Fig. 1c) was recorded. A higher resolution in the TX channel is clearly observed (Fig. 1c), and the contribution of out-of-focus fluorescence light is reduced due to optical sectioning as a consequence of multiphoton absorption [13]. A magnified view on individual microtubule filaments of U373 cells is presented in Figs. 2a and b. The resolution enhancement is further corroborated by the intensity profile (Fig. 2c). Isolated labelled insulas are now clearly discerned.

Beyond biomolecular structures, the  $\sim 2$ -fold resolution enhancement in three dimensions and the optical sectioning achieved with QDTI facilitates quantitative imaging of biomolecular distributions. To demonstrate this finding, we study the distribution of tumour necrosis factor (TNF) receptor 2 (TNFR2) which is located at the plasma membrane. TNFR2 was labelled via immunofluorescence with QDot655 in HeLa cells, and microscopic images were recorded with a conventional confocal microscope (Figs. 3a and b). Tumour necrosis factor alpha (TNF $\alpha$ ) has long been known to be an important mediator of inflammation; its secretion by cells in case of lesions or infections is one of the main events in the cell's response to inflammatory stimuli [14,15]. Activating the TNF receptors 1 (TNFR1) and 2 (TNFR2), the subsequent signal cascade can promote survival, migration, or cell activation, but also cell death, depending on which pathway is set into motion. Both receptors are present on almost all cell types [16], their numbers may vary between 100 and 10,000

receptors per cell [17], expression being dependent on several external stimuli or the cell type, which may play a role in signal transduction [18]. QDTI microscopy of a whole HeLa cell shows the expected enhancement in resolution in the TX channel (Fig. 3b) over the conventional fluorescence channel (Fig. 3a).

To derive quantitative data, we acquired a 3D stack of a HeLa cell and recorded both the emission on the TX channel and the emission of nucleic acid stain Sytox blue. Imaging parameters were set to a pixel size of 90 nm in  $x$  and  $y$  and 190 nm in  $z$ . The distance of  $z$ -planes was chosen with respect to the expected theoretical resolution for three-photon absorption (in the ideal theoretical case), that is, a 3-fold increase over the confocal resolution or  $\sim 200$  nm. A  $z$ -stack projection image recorded with the confocal microscope is presented in Figs. 4a and b. The 3D stack was further analyzed using a spot finding algorithm (ImageJ; NIH), profiting from the bright and well-discernable fluorescence signal of individual quantum dots. With appropriate analytical settings, we determined a total number of  $\sim 21,000$  individual spots (Fig. 4c; magnified view in Fig. 4d and depth-coded view in Fig. 4e). Here, we want to point out that this is not a reliable absolute number of receptors, as we cannot guarantee the efficient and quantitative labelling of each TNFR2 on the cell surface or the robustness of the detection of single quantum dots using the spot finding algorithm. In contrast, we want to demonstrate how QDTI can be used to assess quantitative data on proteins that are too closely spaced to each other to be distinguished by conventional confocal microscopy. Considering a typical cell surface of  $1000 \mu\text{m}^2$  and the resolution limit of confocal microscopy of  $\sim 200$  nm in lateral direction, a quantitative detection of single TNFR2 receptors, which can reach concentrations up to 10,000 proteins per cell [17], would be difficult and ambiguous. QDTI imaging provides a  $\sim 2$ -fold increase in resolution in 3D, which increases the number of detectable receptors by nearly one order of magnitude compared to confocal microscopy. In addition, optical sectioning along the  $z$  axis results in a reduced out-

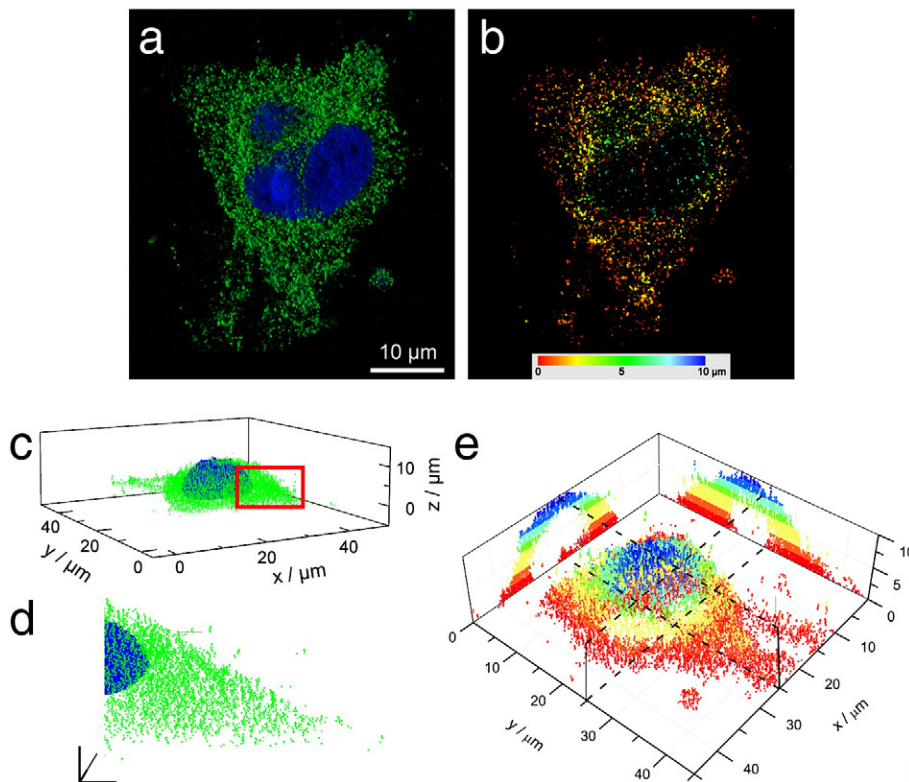


**Fig. 4.** 3D confocal fluorescence images of the triexciton emission channel of quantum dot labelled TNFR2 in a HeLa cell: (a) collapsed view and (b) view with color coding for depth (pixel size in  $x$ ,  $y$ : 90 nm,  $z$ : 190 nm; nucleus labelled with Sytox blue). (c, d) A total number of 21,031 individual TNFR2 receptors were identified on the cell surface using a spot finding algorithm. (e) Reconstructed image with color coding for the  $z$ -coordinate and projections.

of-focus signal such that single and bright emitting quantum dots can be distinguished as single ones. An important fact to consider here is the superior brightness of quantum dots compared to fluorescent proteins or organic fluorophores [19]. This allows using standard confocal microscopes with comparably low irradiation intensities and conventional photomultiplier tubes (PMTs) to detect the fluorescence signal of single quantum dots.

The generation of a triexcitonic state that recombines with fluorescence emission strongly depends on the material of the nanocrystal and the size [11]. So far, QDot655 are the only commercially available quantum dots that exhibit this phenomenon. However, QDTI can be combined with other fluorescent probes, such as organic fluorophores or fluorescent proteins. We demonstrate multicolor and three-dimensional confocal microscopy of COS-7 cells with both the actin cytoskeleton labelled with phalloidin–Alexa Fluor 488 and mitochondrial cytochrome *c* oxidase labelled with QDot655 (Fig. 5a). Cytochrome *c* oxidase is synthesized in the cytoplasm and transported into mitochondria [20], where it is located in the inner mitochondrial membrane and is densely packed. Individual proteins, interprotein distances or structural arrangements are not resolvable with conventional fluorescence microscopy. The resolution that is achieved with QDTI provides, in comparison to the standard fluorescence microscopy, a refined insight on the distribution of cytochrome *c* oxidase in lateral and axial dimensions in mitochondria (Figs. 5b and c). Previously, different techniques that provide subdiffraction resolution have been used to study the mitochondrial inner membrane. A first approach applied 4Pi microscopy [21], a technique that substantially improves the axial resolution down to  $\sim 200$  nm and provided a refined view on three-dimensional mitochondria structure. A second approach used a localization-based superresolution technique and demonstrated to

achieve almost molecular resolution of  $\sim 20$  nm (in the imaging plane) [22]. However, both methods require a more complex experimental procedure as well as expert knowledge, limiting their accessibility. The advantage of QDTI imaging as presented here lies in a simple approach to achieve  $\sim 2$ -fold resolution enhancement in 3D, which is sufficient to address questions on the spatial arrangement of proteins that are not too closely packed.

An important issue to discuss is labeling of biomolecules or biomolecular structures with quantum dots. A first strategy that is applicable to fixed cells is immunofluorescence, as secondary antibodies or antibody fragments labelled with different types of quantum dots are commercially available. However, the size of the quantum dots ( $\sim 10$  to  $20$  nm) and the sandwich complex of antibodies require space. Alternatively, tag-technologies can be used, such as the SNAP-Tag [23], a relatively small protein that is coexpressed to a target protein and which itself can be labelled with specific target molecules. This way, it is possible to introduce a biotin-tag to a protein of interest and, subsequently, label these proteins with quantum dot–streptavidin conjugates. Finally, QDTI is not limited to biomolecular structure or distribution; moreover, tracking of single quantum dots can be combined with triexciton emission, and thus, a higher localization accuracy can be achieved.

#### 4. Conclusion

We have introduced quantum dot triexciton imaging (QDTI) as a method that provides  $\sim 2$ -fold resolution enhancement in three dimensions. QDTI can be realized on any confocal microscope without the need of special equipment, simply requiring continuous-wave laser sources. This new method can be used to image cellular

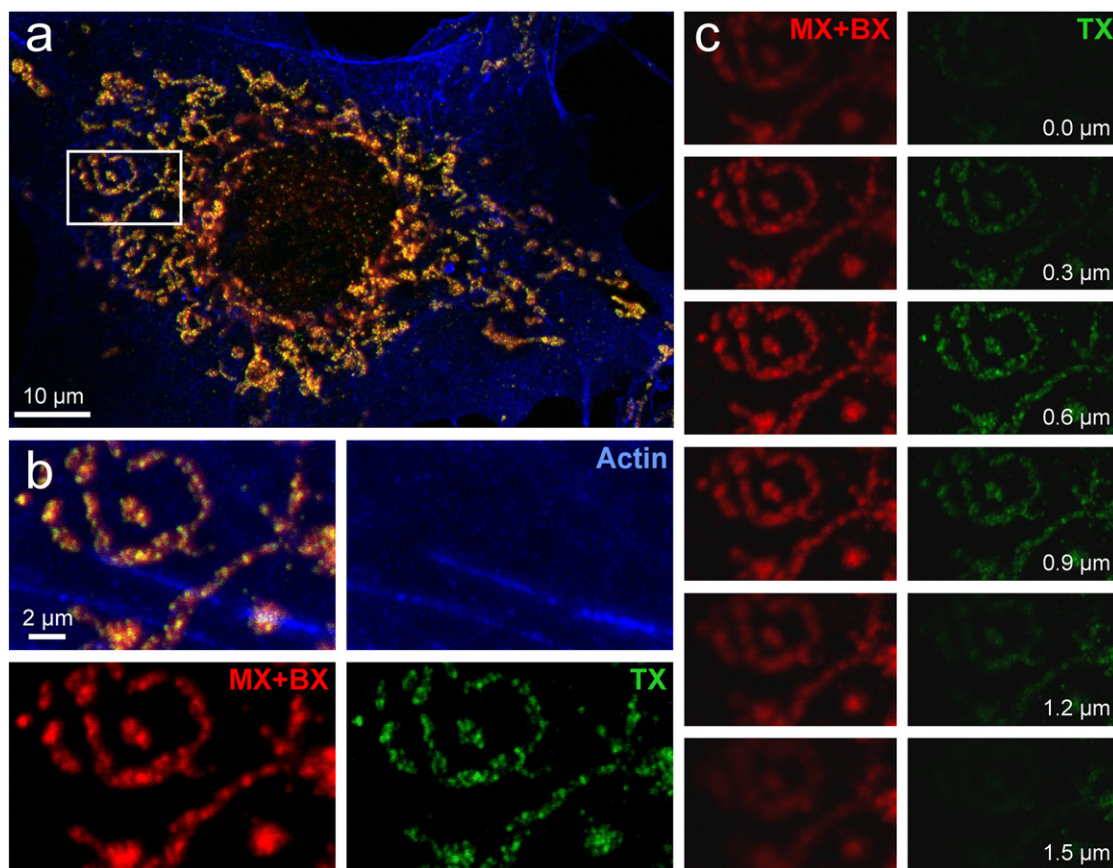


**Fig. 5.** (a) Multicolor confocal fluorescence image of cytochrome *c* oxidase in COS-7 cells labelled with QDot655 (pixel size 63 nm) and actin labelled with phalloidin–Alexa Fluor 488 (excitation wavelengths: 488 nm for Alexa Fluor 488, 543 nm for the TX emission, and 633 nm for the MX emission of QDot655). (b) Magnified view of a mitochondrial structure (pixel size 52 nm). (c) A z-stack scan of the structures in panel b shows both improved lateral and axial resolutions (optical sectioning).

structures and biomolecular distributions and, because of the pure physical nature of the effect, is compatible to live cell experiments.

### Acknowledgment

This work was supported by the Systems Biology Initiative (FORSYS) of the German Ministry of Research and Education (BMBF, grant 0315262).

### References

- [1] S.W. Hell, Microscopy and its focal switch, *Nat. Meth.* 6 (2009) 24–32.
- [2] N. Ji, H. Shroff, H. Zhong, E. Betzig, Advances in the speed and resolution of light microscopy, *Curr. Opin. Neurobiol.* 18 (2008) 605–616.
- [3] M. Heilemann, S. van de Linde, A. Mukherjee, M. Sauer, Super-resolution imaging with small organic fluorophores, *Angew. Chem. Int. Ed Engl.* 48 (2009) 6903–6908.
- [4] M. Heilemann, S. van de Linde, M. Schuttpelz, R. Kasper, B. Seefeldt, A. Mukherjee, P. Tinnefeld, M. Sauer, Subdiffraction-resolution fluorescence imaging with conventional fluorescent probes, *Angew. Chem. Int. Ed Engl.* 47 (2008) 6172–6176.
- [5] H. Shroff, C.G. Galbraith, J.A. Galbraith, E. Betzig, Live-cell photoactivated localization microscopy of nanoscale adhesion dynamics, *Nat. Meth.* 5 (2008) 417–423.
- [6] P. Kner, B.B. Chhun, E.R. Griffis, L. Winoto, M.G. Gustafsson, Super-resolution video microscopy of live cells by structured illumination, *Nat. Meth.* 6 (2009) 339–342.
- [7] V. Westphal, S.O. Rizzoli, M.A. Lauterbach, D. Kamin, R. Jahn, S.W. Hell, Video-rate far-field optical nanoscopy dissects synaptic vesicle movement, *Science* 320 (2008) 246–249.
- [8] S. Hennig, S. van de Linde, M. Heilemann, M. Sauer, Quantum dot triexciton imaging with three-dimensional subdiffraction resolution, *Nano Lett.* 9 (2009) 2466–2470.
- [9] C. Bonati, M.B. Mohamed, D. Tonti, G. Zgrablic, S. Haacke, F. van Mourik, M. Chergui, Spectral and dynamical characterization of multiexcitons in colloidal CdSe semiconductor quantum dots, *Phys. Rev. B* 71 (2005).
- [10] B. Fisher, J.M. Caruge, Y.T. Chan, J. Halpert, M.G. Bawendi, Multiexciton fluorescence from semiconductor nanocrystals, *Chem. Phys.* 318 (2005) 71–81.
- [11] A. Franceschetti, M.C. Tropicovsky, Radiative recombination of triexcitons in CdSe colloidal quantum dots, *J. Phys. Chem. C* 111 (2007) 6154–6157.
- [12] N.R. Ben-Haim, D. Oron, Optical sectioning by multiexcitonic ladder climbing in colloidal quantum dots, *Opt. Lett.* 33 (2008) 2089–2091.
- [13] S.W. Hell, J. Soukka, P.E. Hänninen, Two- and multiphoton detection as an imaging mode and means of increasing the resolution in far-field light microscopy: a study based on photon-optics, *Bioimaging* 3 (1995) 64–69.
- [14] B.B. Aggarwal, Signalling pathways of the TNF superfamily: a double-edged sword, *Nat. Rev. Immunol.* 3 (2003) 745–756.
- [15] D. Widera, A. Kaus, C. Kaltschmidt, B. Kaltschmidt, Neural stem cells, inflammation and NF-kappaB: basic principle of maintenance and repair or origin of brain tumours? *J. Cell. Mol. Med.* 12 (2008) 459–470.
- [16] R.J. Armitage, Tumor necrosis factor receptor superfamily members and their ligands, *Curr. Opin. Immunol.* 6 (1994) 407–413.
- [17] P. Vandenabeele, W. Declercq, R. Beyaert, W. Fiers, Two tumour necrosis factor receptors: structure and function, *Trends Cell Biol.* 5 (1995) 392–399.
- [18] W. Fiers, Tumor necrosis factor. Characterization at the molecular, cellular and in vivo level, *FEBS Lett.* 285 (1991) 199–212.
- [19] M. Bruchez, M. Moronne, P. Gin, S. Weiss, A.P. Alivisatos, Semiconductor nanocrystals as fluorescent biological labels, *Science* 281 (1998) 2013–2016.
- [20] A. Chacinska, C.M. Koehler, D. Milenkovic, T. Lithgow, N. Pfanner, Importing mitochondrial proteins: machineries and mechanisms, *Cell* 138 (2009) 628–644.
- [21] S. Jakobs, High resolution imaging of live mitochondria, *Biochim. Biophys. Acta* 1763 (2006) 561–575.
- [22] S. van de Linde, M. Sauer, M. Heilemann, Subdiffraction-resolution fluorescence imaging of proteins in the mitochondrial inner membrane with photoswitchable fluorophores, *J. Struct. Biol.* 164 (2008) 250–254.
- [23] A. Keppler, S. Gendreizig, T. Gronemeyer, H. Pick, H. Vogel, K. Johnsson, A general method for the covalent labeling of fusion proteins with small molecules in vivo, *Nat. Biotechnol.* 21 (2003) 86–89.
- [24] U. Endesfelder, S. van de Linde, S. Wolter, M. Sauer, M. Heilemann, Subdiffraction-fluorescence microscopy of myosin-actin motility, *Chem. Phys. Chem.* 11 (2010) 836–840.